

# MEMS Microswitches for Reconfigurable Microwave Circuitry

Sean Duffy, Carl Bozler, Steven Rabe, Jeffrey Knecht, Lauren Travis, Peter Wyatt, Craig Keast, and Mark Gouker

**Abstract**—The performance is reported for a new microelectromechanical structure (MEMS) cantilever microswitch. We report on both dc- and capacitively-contacted microswitches. The dc-contacted microswitches have contact resistance of less than  $1\ \Omega$ , and the RF loss of the switch up to 40 GHz in the closed position is 0.1–0.2 dB. Capacitively-contacted switches have an impedance ratio of 141:1 from the open to closed state and in the closed position have a series capacitance of 1.2 pF. The capacitively-contacted switches have been measured up to 40 GHz with  $S_{21}$  less than –0.7 dB across the 5–40 GHz band.

## I. INTRODUCTION

A N RF microelectromechanical (MEMS) switch technology was previously reported for a new class of reconfigurable microwave circuits and antennas [1]. The key advantages of the technology are the compact design of the MEMS cantilever switch and the ability to construct arrays of switches to form distributed, reconfigurable microwave components. The types of components that can be implemented in this technology include filters, impedance matching networks, phase shifters and antennas.

Scanning electron micrographs are shown in Fig. 1 of the dc version of the switch in the open and closed states. The switch is 55  $\mu\text{m}$  long by 45  $\mu\text{m}$  wide and is shown in a coplanar waveguide test circuit. The key to the small switch design is that the pull-down electrode is in the RF path, directly beneath the cantilever (not visible in the figure). To minimize the parasitic effects of the pull down electrode, it is constructed from a high sheet resistance metal. The design presented here is different from other cantilever designs that have the pull-down electrode outside the RF path [2], [3]. Further, the design presented here does not need auxiliary structures like the support posts and spring mechanisms found in membrane switch designs [4]–[6].

Scanning electron micrographs are shown in Fig. 1 of the capacitive version of the switch in the open and closed states. This switch is larger than the dc version in order to achieve the level of capacitance required for microwave applications. The switch is 200  $\mu\text{m}$  long and 148  $\mu\text{m}$  wide, and the capacitive area is 46  $\mu\text{m}$  by 148  $\mu\text{m}$  with a 150 nm thick silicon dioxide forming the parallel plate capacitor. Three corrugations (4  $\mu\text{m}$  by 148  $\mu\text{m}$ ) are formed in the flat parallel plate region to provide

Manuscript received August 14, 2000; revised December 18, 2000. This work was supported by the Defense Advanced Research Projects Agency under Air Force Contract F19628-00-C-0002. Opinions, interpretations, recommendations, and conclusions are those of the authors and are not necessarily endorsed by the United States Air Force.

The authors are with MIT Lincoln Laboratory, Lexington, MA 02420-9108 (e-mail: [sduffy@ll.mit.edu](mailto:sduffy@ll.mit.edu)).

Publisher Item Identifier S 1531-1309(01)03044-6.

additional strength and stability. The other design features of this switch are the same as just described for the dc switch.

Device results are presented in Section III for both types of microswitch. Capacitively-contacted microswitches with cPa-capacitance values of 1.2 pF are measured in the closed state while open state capacitance of 8.5 fF is observed. The  $S_{21}$  is less than –0.7 dB from 5 to 40 GHz. The dc switches have been measured with dc resistances of as low as  $0.6\ \Omega$  and the RF performance of several low contact resistance switches are demonstrated with an  $S_{21}$  of –0.1 to –0.2 dB from 0.2 to 40 GHz.

## II. DEVICE TECHNOLOGY

The RF microswitches are fabricated using silicon CMOS processing techniques. The cantilever arm is formed from a three-layer deposition of 350 nm aluminum sandwiched between two 100 nm layers of controlled-stress silicon dioxide. The materials for the switch were chosen because silicon dioxide is strong and resilient and has low density, low Young's modulus and low thermal expansion coefficient. This combination balances the high-expansion aluminum and provides stability over temperature. In the resting state, the built-in stresses of the silicon dioxide films curl the switch arm away from the substrate so that the switch contact is open, and the RF impedance is high. The curling motion of the cantilever arm allows the microswitch to be very compact, while at the same time providing a relatively large open-contact separation distance,  $\sim 10\text{--}15\ \mu\text{m}$ , and thus relatively high on–off capacitance ratios. The placement of the platinum contacts and the pattern definition of an etch step determines whether the microswitch is capacitively or dc contacted, and these devices can be used side-by-side in a circuit design. A platinum-to-platinum contact is used for the dc contact, since it does not form an oxide and is less likely to promote stiction. A high resistivity electrode (Ta<sub>N</sub>) (50 k $\Omega$ /sq) is buried 200 nm below the switch. Application of a voltage between the switch and the electrode results in an electrostatic force that pulls the switch cantilever into contact with the substrate in a rolling motion.

The SEM photographs of the open and closed-state positions of the switch shown in Fig. 1 reveal some of the key design innovations. The fabrication process permits formation of corrugations in the membrane, which can be used to adjust the stiffness of the cantilever arm and contact region. Corrugations have been incorporated in the cantilever arm where it attaches to the substrate to provide strain relief. The process also permits the modification of the details of the contact region so that varying size and density of dc contact dimples can be formed. Nominal designs range from ten 2- $\mu\text{m}$  contact dimples to three 8- $\mu\text{m}$  contact dimples in the contact region.

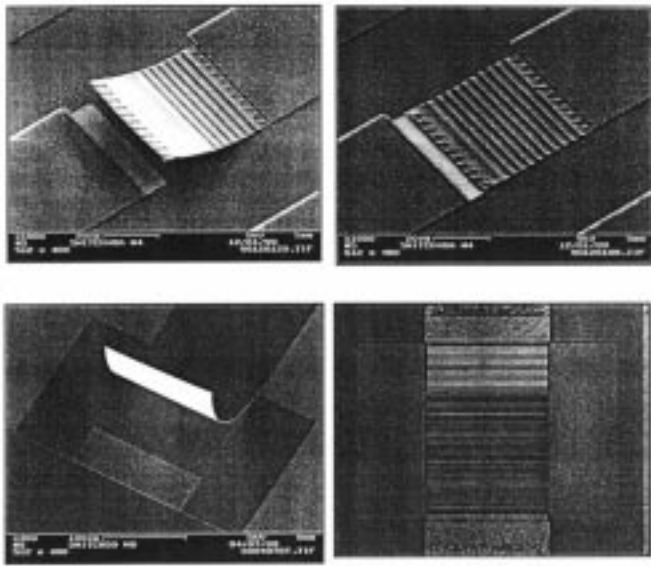


Fig. 1. SEM photograph of open and closed state of cantilever switch. Top: dc contacted switch, bottom: capacitively-contacted switch.

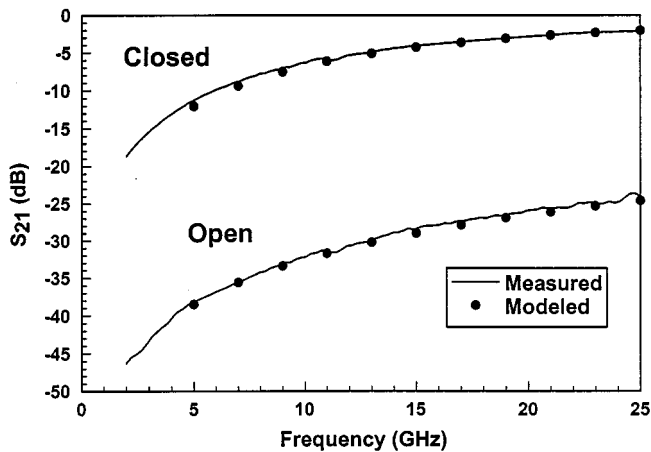


Fig. 2. Measured and calculated  $S_{21}$  for the small capacitive switch.

Switches are currently fabricated on high resistivity 3000  $\Omega$ -cm silicon with a thickness of 675  $\mu$ m. This substrate is not ideal for microwave and millimeter wave operation due to high line and surface wave losses compared to thinner, lower dielectric constant substrates. Future work will include constructing the microswitches on substrates with better RF performance using either a thinner silicon or quartz substrate.

### III. DEVICE RESULTS

Measurements on two capacitively-contacted switch designs in coplanar waveguide (CPW) show close agreement with calculations. The first design was identical to the dc switches except that the contacts were replaced with a parallel plate overlap region of 8 by 45  $\mu$ m and having 150 nm of silicon dioxide between the metal of the switch and the metal on the substrate. Open-state performance was measured and compared to calculations in Fig. 2 using HFSS [7]. The value of the open-state

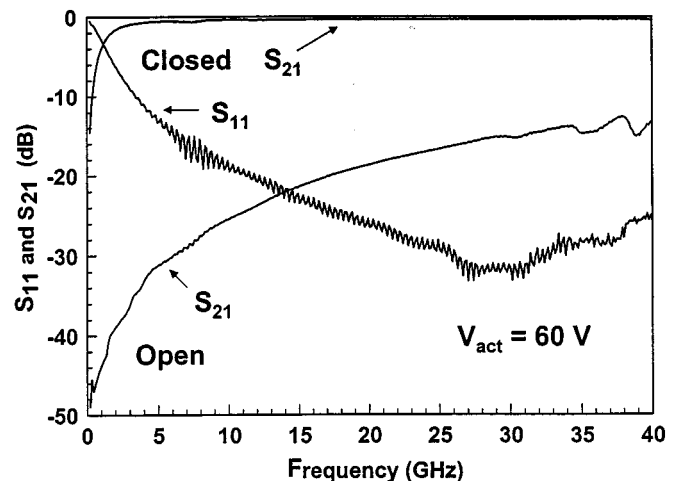


Fig. 3. Open and closed state measurement of the large capacitive switch.

capacitance, 4 fF, was found by a curve fit of the calculations to an ideal series capacitor in a 50-ohm transmission line. Predictions for the closed state use the simple parallel plate capacitor equation,  $C = \epsilon_r \epsilon_0 A/d$ , where  $\epsilon_r = 3.9$  for  $\text{SiO}_2$ ,  $A$  is the area of the parallel plate region and  $d$  is the oxide thickness. The  $S_{21}$  for the model and the measured results of the closed state are given in Fig. 2. The predicted closed state capacitance of 83 fF shows close agreement to the measured data. However, the small closed state capacitance makes this small contact area switch design of little practical use at microwave frequencies.

A second capacitive switch design more suitable for microwave applications was fabricated and measured. This switch is a larger, 200 by 148  $\mu$ m, with an overlap region of 46 by 148  $\mu$ m and a 150 nm oxide thickness. The measured results are given in Fig. 3 for a switch in 50  $\Omega$  CPW and include a 500  $\mu$ m section not de-embedded in the data. The predicted closed state capacitance is 1.21 pF (removing the corrugation regions from the calculation) and shows close agreement to measurement. Curve fits to the measured data show a closed state capacitance of 1.2 pF and an open state capacitance of 8.5 fF leading to a capacitance on/off ratio of 141. The  $S_{21}$  is  $-0.5$  dB at 5 GHz,  $-0.3$  dB at 25 GHz, and  $-0.7$  dB at 40 GHz. The crossover frequency of  $S_{11}$  and  $S_{21}$  for a series capacitor is  $f_c = (4\pi C Z_o)^{-1}$  which results in a predicted crossover at 1.3 GHz, close to the 1.2 GHz seen in Fig. 3. Failure-free operation for power levels tested up to 2 W at 10 GHz has been observed for the capacitively-contacted switch. Operation at power levels above 2 W has not been measured yet.

Several different versions of the contact and cantilever design of the dc switch shown in Fig. 1 have yielded consistently low contact resistance. On the best device design a number of wafers were tested with a 60% yield below 1  $\Omega$  and 90% yield below 2  $\Omega$  for the contact resistance. Even though actuation of the switch occurs at around 35 V, it was found that low resistances were achieved only when the voltage was increased to 80 V. In these device measurements, the actuation voltage is applied through an off-chip bias network. On-chip methods using a second electrode have also been used successfully. Measurements of the

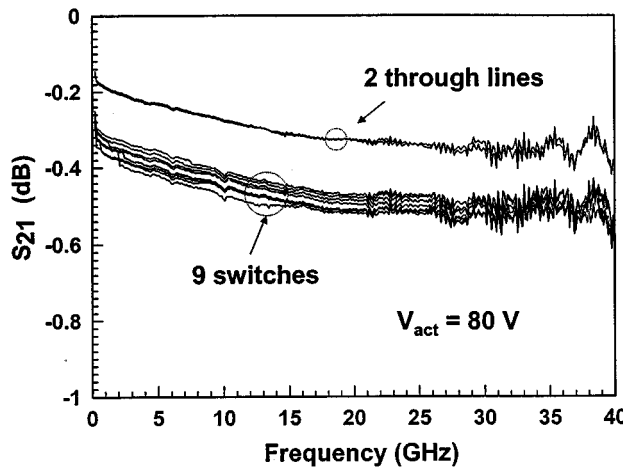


Fig. 4. Closed state  $S_{21}$  of nine dc switches and the line loss of the CPW test through line.

dc switch from 0.2–40 GHz are shown in Fig. 4. The inherent loss in the CPW line is included in the measured results for the switch. Removing this loss from the switch result yields a relatively constant switch loss of 0.1–0.2 dB consistent with the constant loss prediction of a real resistance [ $S_{21} = 2Z_o/(2Z_o + R_s)$  where  $R_s$  is the switch resistance and  $Z_o$  is the line impedance]. These RF results demonstrate switch resistances between 1 and 2  $\Omega$ .

The capacitance of the open state of the dc switch is identical to the capacitive switch of Fig. 2. The capacitance of the open state has been calculated as a function of switch angle and height and is illustrated in Fig. 5. When the switch height becomes large, the capacitance becomes dominated by substrate coupling which is fairly high for the 675  $\mu\text{m}$  silicon substrate. A simple method of reducing the open state capacitance of the switch is to fabricate or transfer the switch to a thin quartz substrate or suspended transmission line. This would not affect the closed state performance and the capacitance on/off ratio would rise accordingly. When the switch gets close to the metal on the substrate, the closed state becomes dominated by the parallel plate capacitance. Typical release heights are shown on Fig. 5. The small variation in capacitance versus the typical heights provides some robustness for minor process deviations.

Switch speeds for the dc switch are under 1  $\mu\text{s}$  for open and close times. The switch speed for the large capacitive device is somewhat slower, 3  $\mu\text{s}$  for the close time and approximately 20  $\mu\text{s}$  for the open time. Reliability testing is ongoing, how-

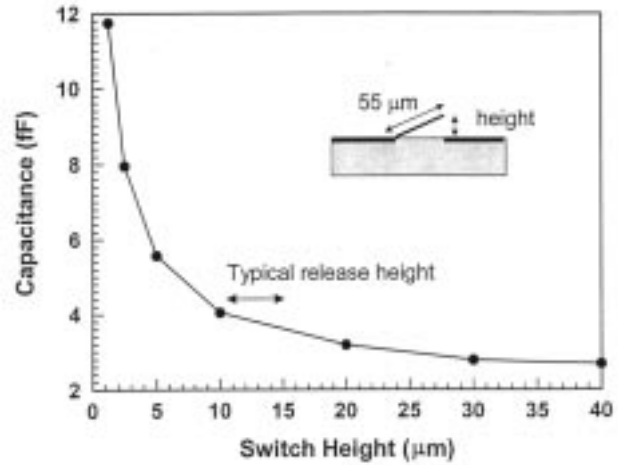


Fig. 5. HFSS calculation of open state capacitance for switch at varying heights.

ever, similar device designs have been operated for  $10^9$  cycles without failure and over a  $-70^\circ\text{C}$ – $170^\circ\text{C}$  temperature range in an optical display application.

#### IV. CONCLUSION

A novel MEMS microswitch device has been presented with measured results. The dc and capacitively-contacted switches have RF performance comparable to or better than pin diode switches and other MEMS switches.

#### REFERENCES

- [1] C. Bozler, R. Drangmeister, S. Duffy, M. Gouker, J. Knecht, L. Kushner, R. Parr, S. Rabe, and L. Travis, "MEMS microswitch arrays for reconfigurable distributed microwave components," in *IEEE 2000 IMS Dig.*, 2000, pp. 200–204.
- [2] P. M. Zavacky, N. E. Gruer, R. H. Morrison, and D. Potter, "Microswitches and microrelays with a view toward microwave applications," *Int. J. RF Microw. CAE*, vol. 9, no. 4, pp. 338–347, 1999.
- [3] D. Hyman, J. Lam, B. Warneke, A. Schmitz, T. Y. Hsu, J. Brown, J. Schaffner, A. Walston, R. Y. Loo, M. Mehregany, and J. Lee, "Surface-micromachined RF MEMS switches on GaAs substrates," *Int. J. RF Microw. CAE*, vol. 9, no. 4, pp. 348–361, 1999.
- [4] C. L. Goldsmith, A. Malczewski, Z. J. Yao, S. Chen, J. Ehmke, and D. H. Hinzel, "RF MEMS variable capacitors for tunable filters," *Int. J. RF Microw. CAE*, vol. 9, no. 4, pp. 362–374, 1999.
- [5] J. B. Muldavin and G. M. Rebeiz, "30 GHz tuned MEMS switches," in *IEEE 1999 IMS Dig.*, 1999, pp. 1511–1514.
- [6] S. Pacheco, C. T. Nguyen, and L. P. B. Katehi, "Micromechanical electrostatic K-band switches," in *IEEE 1998 IMS Dig.*, 1998, pp. 1569–1572.
- [7] High frequency structure simulator, v. 5.4, Agilent Technologies, Santa Rosa, CA.